

# Low- $J$ rotational spectra, internal rotation, and structures of several benzene-water dimers

H. S. Gutowsky, T. Emilsson, and E. Arunan  
*Noyes Chemical Laboratory, University of Illinois, Urbana, Illinois 61801*

(Received 24 May 1993; accepted 14 June 1993)

Low  $J$  (0–4) rotational transitions have been observed for the benzene–water dimer of which high  $J$  ( $\geq 4$ ) transitions were reported recently by Blake [Science **257**, 942 (1992)]. Our experiments used a modified Balle/Flygare Fourier transform microwave spectrometer, with a pulsed supersonic nozzle as the sample source, and examined a variety of isotopic species in the ground and first excited internal rotor states ( $m=0$  and 1). The dimers of the parent  $C_6H_6$  benzene with  $H_2O$ , HDO,  $D_2O$ , and  $H_2^{18}O$  have symmetric top spectra characteristic of two coaxial rotors with a symmetric top frame and a very low effective  $V_6$  barrier. The dimers of  $H_2O$  and  $D_2O$  with the  $^{13}C$  and  $D$  monosubstituted benzenes have asymmetric top spectra of which only the  $m=0$  state was assigned. However, doublets in the  $m=1, J=0 \rightarrow 1$  transitions show that there is a  $V_2$  term of  $\sim 0.5$  MHz in their barriers. A substitution analysis was made of the rotational constants found for the  $m=0$  state of the dimers with  $H_2^{18}O$ ,  $D_2O$ , and the  $^{13}C$  and  $D$  monosubstituted benzenes. It shows that the oxygen is at the  $a$  axis of the dimer, well outside (0.48 Å) the hydrogens. However, the  $C_2$  axis of the  $H_2O$  is not coincident with the  $a$  axis but is at an angle  $\beta$  of  $37^\circ$  to it, rotated so that the two hydrogens are equivalent. The sixfold axis of the benzene corresponds to the  $a$  axis, there is little or no tilt ( $\gamma$ ) of the benzene. The c.m. ( $C_6H_6$ ) to c.m. ( $H_2O$ ) distance  $R$  is 3.329 Å. The closely spaced hyperfine structure from the proton–proton magnetic dipole interaction and the deuterium quadrupole interaction was resolved for several dimers and transitions, principally  $J=0 \rightarrow 1$  and  $1 \rightarrow 2$ . The results demonstrate effective nuclear equivalence in dimers with  $H_2O$  and  $D_2O$ . Also, the symmetries found for their nuclear spin functions correlate with the lowest rotational levels of free water, the  $m=0$  state with  $0_{00}$  and  $m=1$  with  $1_{01}$  and  $1_{11}$ . For the  $m=1, K=0$  transitions of  $C_6H_6-H_2O$  the correlation is with  $1_{11}$  and for the  $K=\pm 1$ , with  $1_{01}$ . These assignments are reversed for  $C_6H_6-D_2O$ .

## INTRODUCTION

Liquid benzene and water are relatively immiscible. In molecular terms this implies that both the benzene–benzene and water–water interactions are much stronger than the benzene–water interactions. The differences in the weak intermolecular forces should be more directly evident in the structure, energetics, and dynamics of small homo- and hetero-molecular clusters  $(C_6H_6)_m(H_2O)_n$ . In particular, the bulk properties of the benzene–water system should derive largely from the molecular properties of the water–water, benzene–benzene, and water–benzene dimers, trimers, and larger groupings. The present work seeks to study the intermolecular interactions of benzene and water through observations of rotationally resolved spectra which are now available for small clusters by several methods using the seeded supersonic jet to generate the desired species.<sup>1</sup>

The weakness and consequent near isotropy of the interactions within a cluster allows a wide range of large amplitude motions to occur in them. Their characterization is a formidable task, often requiring extensive observations of vibration–rotation–tunneling (VRT) spectra combined with permutation–inversion (PI)<sup>2</sup> and potential energy surface (PES)<sup>3</sup> theoretical analysis. Of the three dimers in the benzene/water system only the water dimer has been analyzed at this level of detail, in work extending over more than a decade.<sup>4</sup> In the case of the benzene–water

dimer, the observation of high  $J$  ( $J=4$  to 10) rotationally resolved spectra was reported recently by Blake's group,<sup>5</sup> while a preliminary account has been given elsewhere by us of the rotational spectrum for the benzene–benzene dimer.<sup>6</sup>

Here the focus is on the benzene–water dimer for which we have studied the low- $J$  (0 to 4) rotational transitions at high resolution. The primary species of the dimer is a *symmetric* top with the  $H_2O$  in effect on the sixfold axis of the benzene with little or no barrier to internal rotation about that axis. The covalently bonded methylsilylacetylene is an analogous system which is inherently a symmetric top. It was first treated in detail by Kirchhoff and Lide<sup>7</sup> and later adapted by Fraser *et al.* to the  $CF_3H-NH_3$  dimer.<sup>8</sup> In the centrifugal distortion notation of Fraser the transition frequencies are given by the expression

$$\nu = 2(J+1)\{B - D_{JK}K^2 - D_{Jm}m^2 - D_{JKm}Km - H_{JKm}m^2K^2\} - 4(J+1)^3 D_J. \quad (1)$$

The internal rotation state is specified by the quantum number  $m=0, \pm 1, \dots$ , while the symbols with  $D$  or  $H$  are centrifugal distortion constants.

We have found the major features of the rotational spectra for  $C_6H_6-H_2O$ ,  $-D_2O$ , and  $-H_2^{18}O$  to be fitted by Eq. (1) with  $m=0$  and 1. If  $m=0$ , Eq. (1) reverts to the usual  $K^2$  progressions at each  $J$  for a semirigid symmetric top.<sup>9</sup> These  $m=0$  transitions of the  $H_2O$ ,  $D_2O$ , and HDO isotopic species for the dimer were first observed and fitted

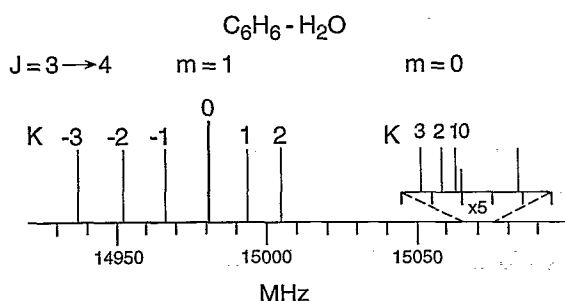


FIG. 1. Stick diagram of the  $J=3 \rightarrow 4$  symmetric top transition observed for the  $C_6H_6-H_2^{18}O$  dimer, including  $m=0$  and  $m=1$  internal rotor states. The strong unlabeled component at the far right is found for all  $J \rightarrow J+1$  transitions with  $J > 0$ . It occurs at the apparent expense of the  $m=1, K=+J$  component, which is otherwise missing.

by Blake.<sup>5</sup> A second, more extensive set of progressions is described by  $m=1$ , as shown in Fig. 1 and considered in detail later on. The structural implications of the fits to Eq. (1) are considerable. Both the  $m=0$  and  $m=1$  states appear to be symmetric tops even though a classical snapshot of the dimer would find the water molecule to be a highly asymmetric top.

Intuitively, this behavior seems compatible with the high rotational and translational mobility shown for the water in the dimer by theoretical studies<sup>3,5</sup> of its potential energy surface (PES). Moreover, internal rotation theory predicts symmetric top spectra for coaxial rotors of six- and twofold symmetry with a small effective barrier.<sup>10</sup> In order to develop a better understanding of this phenomenon, we have observed the rotational spectra of several dimers with isotopic species of lower symmetry,  $C_6H_5D$ ,  $C_5^{13}CH_6$ , or HDO. Analysis of the results discloses remarkable diversity in the dynamics of the dimers.

## EXPERIMENT

The rotational transition frequencies were measured with the Balle/Flygare Mark II FT-MW spectrometer which has a pulsed supersonic nozzle and large Fabry-Perot cavity as previously modified and described.<sup>11</sup> Neon first run (70% Ne and 30% He) was generally used as the carrier gas, giving somewhat stronger signals than He alone or Ar. A backing pressure of 1 to 1.5 atm was customary for the carrier gas which was seeded by passing 1% of the carrier through a benzene bubbler and 2% through a water bubbler, both at ambient temperatures. The nozzle has an orifice 1 mm in diameter and the microwave pulse was usually 0.3  $\mu$ s in duration.

The signals were quite strong, especially considering the very large number of transitions present. The signal acquisition time was typically 10 to 20 s. The accuracy of the frequencies reported was often limited by unresolved hyperfine structure (hfs) caused by proton-proton, magnetic dipole-dipole interactions in the benzene. The frequencies measured usually have a standard deviation of less than a kHz.

The gases and chemicals used were obtained from a variety of sources as follows: Ar (Liquid Air), He

(Linde), Ne first run (Airco),  $C_6H_6$  (Fisher),  $D_2O$  (Sigma),  $^{13}C$  depleted benzene with 99.95%  $^{12}C$  (Cambridge Isotope Laboratories),  $H_2^{18}O$  with 92.5%  $^{18}O$  (Isotec, Inc.). The monodeutero benzene was synthesized in our laboratory by the reaction of  $D_2O$  with a 3M solution of phenyl magnesium bromide in ethyl ether (Aldrich). The isotopic purity of the fractionally redistilled product  $C_6H_5D$  was determined mass spectrometrically to be 98%.

## RESULTS AND ANALYSIS

### Assignments and rotational constants

Our introduction to the benzene-water system was aided substantially by the Dykstra and Blake groups. From the former, Augspurger provided us with a preprint of their MMC paper on the interaction potential for the dimer,<sup>3</sup> augmented with several sets of representative rotational constants. Blake later gave us the  $\bar{B}$  value they had found by fitting the  $K=0$  transitions at higher  $J$  (4 to 10) for what later proved to be a symmetric top, the  $m=0$  state of the  $C_6H_6-H_2O$  dimer. Moreover, Suzuki kept us well informed about the progress of their work. Especially helpful were a prediction of the low- $J$  (0 to 4) transitions for the parent symmetric top, preprints of early and final drafts of their Science article,<sup>5</sup> and extensive listing for "clumps" of unassigned transitions they had observed at higher  $J$ .

Identification and assignment of transitions in the benzene/water system is a challenge. Many regions in our spectral range (2.5 to 18.6 G) are heavily congested by this system, for which it is not uncommon to find several transitions within a MHz. In addition to a prolific variety of benzene/water heterospecies with complex spectra, the benzene homodimer also contributes profusely.<sup>6</sup> The parent water dimer has only a few transitions in this region but those from dimers with HDO and  $D_2O$  are more common and less well cataloged;<sup>4</sup> also, larger clusters undoubtedly appear. Ordinarily, species with  $^{13}C$  at natural abundance (1.1%) are not much of a problem, but with 7% of the benzene as  $C_5^{13}CH_6$  it generates a lot of weak, asymmetric top transitions. Also, although the use of neon first run as carrier gives the strongest benzene/water signals and He is a very poor cluster former, some of the transitions require Ne. Among them we have identified a Ne- $C_6H_6-H_2O$  symmetric top trimer which will be reported later.

Care was taken to obtain correct assignments. Intensity and the lack or presence of hfs were good preliminary indicators. More weight was given to the effect upon a signal of cutting off each of the sampler bubblers separately or of changing the carrier gas. A critical test of each benzene-water transition was to substitute  $^{13}C$  depleted benzene for ordinary benzene to identify the isotopic species of benzene responsible for that transition. The gas handling system in use is designed to enable such checks to be made readily.<sup>12</sup> The main problem with it in the present case is the tendency of water to degas forever from almost every surface.

TABLE I. Observed and fitted rotational transition frequencies for benzene-water dimers with  $m=0$  free internal rotor, symmetric top ground states.

Transition	$J \rightarrow J'$	$K$	$C_6H_6-H_2O$		$C_6H_6-D_2O$		$C_6H_6-H_2^{18}O$		$C_6H_6-HDO$	
			Obs. (MHz)	Res. <sup>a</sup> (kHz)	Obs. (MHz)	Res. (kHz)	Obs. (MHz)	Res. (kHz)	Obs. (MHz)	Res. (kHz)
0→1	0	0	3 989.5358	2.1	3 824.0122	-0.2	3 767.4105	1.2	3 912.5937	-2.4
1→2	1	1	7 978.8352	0.0	7 647.7535	2.8	7 534.5994	0.1	7 824.8739	6.9
		0	8.9869	0.1	7.9331	-3.8	4.7426	0.0	5.1021	-6.8
2→3	2	1	11 967.3685	-0.5	11 470.5710	2.7	11 301.0635	-0.7	11 736.0101	6.1
		2	8.0508	-0.7	1.4060	-0.1	1.7079	-0.9	7.0924	0.1
		0	8.2785	-0.5	1.6841	-1.3	1.9244	0.7	7.4504	-4.7
3→4	3	1	15 954.6008	1.0	15 291.8178	-1.0	15 066.2989	0.7	15 645.1958	-2.4
		2	6.1150	-1.4	3.6804	-0.1	7.7299	-0.7	7.6166	-0.1
		1	7.0250	-1.3	4.7979	0.4	8.5898	-0.3	9.0680	0.3
		0	7.3320	2.4	5.1702	0.3	8.8772	0.7	9.5530	1.6

<sup>a</sup>Res. = Obs. - Calc.

### Symmetric tops

The main transitions of the symmetric ( $D_{6h}/C_{2v}$ ) benzene/water dimers are quite characteristic, once spotted. At each  $J$  they form two strong progressions, for  $m=0$  and  $m=1$ , as described by Eq. (1) and shown in Fig. 1 for the  $J=3 \rightarrow 4$  spectrum of  $C_6H_6-H_2^{18}O$ . The  $m=0$ , symmetric top progression<sup>9</sup>  $2(J+1)D_{JK}K^2$  occurs at higher frequencies, its components separated by that term from the  $K=0$  component. An ordinary value of 35.8 kHz is found for  $D_{JK}$ . The  $K=0$  component of the  $m=1$  state is  $2(J+1)D_{Jm}m^2$  or 91 MHz below the  $K=0$  components for the  $m=0$  progression. The  $m=1$  progression is characteristic of a symmetric top with a free internal rotor.<sup>8</sup> It consists essentially of  $2J+1$  components displaced symmetrically by  $2(J+1)D_{JKm}Km$  from the  $K=0$  center. This lifting of the  $K \pm$  degeneracy leads to a sign ambiguity in designating the components, where we have arbitrarily assigned  $m = +1$  rather than  $-1$ . Actually the spacings ob-

served in the  $m=1$  progressions decrease systematically at higher frequency, a trend accommodated by the small term  $-2(J+1)(D_{JK} + H_{JKm}m^2)K^2$ .

Progressions of this nature were found for three isotopomers of the benzene-water dimer, the parent  $^{12}C_6H_6$  benzene with  $H_2O$ ,  $D_2O$ , and  $H_2^{18}O$ . Their assigned frequencies are listed in Tables I and II for  $m=0$  and  $m=1$ , respectively. For HDO only the  $m=0$  progression was found. In separate trial fits of the two progressions different values were obtained for  $D_J$ , the value being negative for  $m=1$ . This was accommodated by replacing  $D_J$  in Eq. (1) with the  $m$ -dependent term  $(D_J - D_{Jm}m^2)$ . Simultaneous fits for  $m=0$  and  $m=1$  led to the rotational constants listed in Table III. Our results for the low- $J$ ,  $m=0$  progressions differ slightly from those reported by Blake for the high- $J$  progressions<sup>5</sup> of  $C_6H_6-H_2O$  and  $C_6H_6-D_2O$ . The residues of our fits are included in Tables I and II; the rms deviations ( $\sigma$ ) are given separately for  $m=0$  and 1 in

TABLE II. Observed and fitted rotational transition frequencies in MHz for benzene-water dimers with  $m=1$  first excited free internal rotor, symmetric top states.

Transition <sup>a</sup>	$J \rightarrow J'$	$K$	$C_6H_6-H_2O$		$C_6H_6-D_2O$		$C_6H_6-H_2^{18}O$	
			Obs.	Res.	Obs.	Res.	Obs.	Res.
0→1	0	0	3 963.2947	-0.1948	3 765.534	1.364	3 744.5118	-0.1669
1→2	-1	1	7 919.7245	0.1211	7 511.852	4.014	7 482.9140	0.1488
		0	26.9889	-0.2522	533.679	-2.036	9.3227	0.2479
		1	81.4323	<sup>b</sup>	656.735	<sup>b</sup>	536.6581	<sup>b</sup>
2→3	-2	2	11 868.1338	0.4135	11 252.689	<sup>b</sup>	11 214.1667	0.4134
		-1	79.9854	-0.0748	281.880	-0.178	24.6511	-0.0297
		0	91.4670	-0.0498	307.499	1.775	34.7376	-0.1515
		1	905.1077	<sup>b</sup>	334.499	-0.310	47.1562	<sup>b</sup>
		2	71.9417	<sup>b</sup>	484.885	<sup>b</sup>	304.7959	<sup>b</sup>
3→4	-3	3	15 807.3407	0.1216	15 016.268	-0.456	14 937.2120	0.0755
		-2	15 824.5635	-0.2865	35.429	1.600	52.4651	-0.2088
		-1	40.7324	-0.5707	58.234	0.075	66.7357	-0.5003
		0	57.1318	0.5512	88.179	-1.536	81.0596	0.2129
		1	70.9703	0.3140	102.046	<sup>b</sup>	94.1603	0.6623
		2	84.3623	-0.2341	141.306	<sup>b</sup>	15 004.8573	-0.3327
		3	962.2039	<sup>b</sup>	312.762	<sup>b</sup>	72.9016	<sup>b</sup>

<sup>a</sup>This choice of signs for  $K$  leads to the signs given for  $m$  and  $D_{JKm}$ .<sup>b</sup>Not included in the fit. See the text.

TABLE III. Rotational constants determined by fitting to Eq. (1) the transitions observed for benzene-water dimers with symmetric top,  $m=0$  and  $m=1$  internal rotor states.

Constant <sup>a</sup>	C <sub>6</sub> H <sub>6</sub> -H <sub>2</sub> O	C <sub>6</sub> H <sub>6</sub> -HDO	C <sub>6</sub> H <sub>6</sub> -D <sub>2</sub> O	C <sub>6</sub> H <sub>6</sub> -H <sub>2</sub> <sup>18</sup> O
	<i>m=0 state</i>			
<i>B</i> (MHz)	1994.7735(2)	1956.305(1)	1912.0135(3)	1883.7110(1)
<i>D<sub>J</sub></i> (kHz)	3.354(1)	3.47(3)	3.66(1)	3.170(5)
<i>D<sub>JK</sub></i> (kHz)	37.91(2)	60.46(8)	46.54(4)	35.81(1)
<i>σ</i> (kHz)	1.3	4.0	1.8	0.7
	<i>m=1 state</i>			
<i>D<sub>Jm</sub></i> (MHz)	13.05(7)		29.7(3)	11.39(6)
<i>D<sub>JKm</sub></i> (MHz)	-1.84(1)		-4.37(12)	-1.64(1)
<i>H<sub>JKm</sub></i> (kHz)	35.7(73)		498.(58)	24.(7)
<i>D<sub>JIm</sub></i> (kHz)	14.(3)		140.(10)	12.(2)
<i>σ</i> (MHz)	0.32		1.75	0.32

<sup>a</sup>The numbers in parentheses are the standard deviation.

Table III. For  $m=0$ , the  $\sigma$ 's are 1 to 4 kHz, within the experimental error for the various isotopic species. However, for  $m=1$  the  $\sigma$ 's are 0.3 MHz for H<sub>2</sub>O and H<sub>2</sub><sup>18</sup>O, 300-fold larger, indicating a deficiency in the model used to fit the  $m=1$  data. The even larger  $\sigma$  for C<sub>6</sub>H<sub>6</sub>-D<sub>2</sub>O of 1.75 MHz is caused by spectral congestion, weak signals, and associated assignment ambiguities.

An interesting feature of the three symmetric top species with  $m=1$  states is evident in Fig. 1 and Table II. In each of their  $J \rightarrow J+1$  transitions with  $J > 0$  the predicted highest frequency component ( $K=+J$ ) is missing in the progression. Instead, there is a strong transition several MHz above the  $K=0$  line for the  $m=0$  progression. Also, the  $J=2 \rightarrow 3$ ,  $K=1$  component of the  $m=1$  progressions, adjacent to the "missing"  $K=2$  component, is displaced but only a MHz or so instead of 50. The frequencies of the three displaced  $K=J$  lines were fitted for each isotopic species as  $K=0$  transitions, giving the values for  $B$  and  $D_J$  listed in Table IV. The results correspond closely to those for the  $m=0$  symmetric top fits in Tables I and III.

In the case of the dimer with HDO, Blake *et al.*<sup>5</sup> found only  $m=0$  transitions at high  $J$ , behavior analogous to that reported by Fraser *et al.* for the Ar/H<sub>2</sub>O system.<sup>13</sup> The absence of the  $m=1$  transitions was attributed to relaxation in the jet expansion of the metastable  $m=1$  species to the  $m=0$  state, a process predicted to be<sup>2</sup> nuclear-spin forbidden in the homonuclear dimers of benzene with H<sub>2</sub>O and D<sub>2</sub>O but allowed for HDO. Similar effects have been

TABLE IV. Frequencies of the  $K=+J$  components displaced from the  $m=1$  progressions in Table II and their fit as  $K=0$  transitions.

Transition $J \rightarrow J+1$	C <sub>6</sub> H <sub>6</sub> -H <sub>2</sub> O (MHz)	C <sub>6</sub> H <sub>6</sub> -D <sub>2</sub> O (MHz)	C <sub>6</sub> H <sub>6</sub> -H <sub>2</sub> <sup>18</sup> O (MHz)
1→2	7 981.4323	7 656.7354	7 536.6581
2→3	11 971.9417	11 484.8848	11 304.7959
3→4	15 962.2039	15 312.7617	15 072.7016
Constant (Units)			
<i>B</i> (MHz)	1 995.3856(1)	1 914.2154(6)	1 884.1903(2)
<i>D<sub>J</sub></i> (kHz)	3.440(2)	3.76(2)	3.204(6)

noted by Gotch and Zwier.<sup>2</sup> We too found only  $m=0$  transitions of C<sub>6</sub>H<sub>6</sub>-HDO. Their frequencies and rotational constants are included in Tables I and III. The rms deviation of the fit is 4 kHz, a bit larger than normal, probably because of the partially resolved hyperfine structure. Our low- $J$  values for the rotational constants are consistent with those reported for high  $J$ .<sup>5</sup>

Also with C<sub>6</sub>H<sub>6</sub>-HDO, we did not observe the strong lines found just above the  $m=0$  progressions for the dimers with H<sub>2</sub>O and D<sub>2</sub>O (Fig. 1). This is indirect evidence for assigning the latter to the  $m=1$  progression.

### Asymmetric tops

The transitions of the benzene/water dimers were examined for two asymmetric benzenes, the monodeutero and mono <sup>13</sup>C isotopomers, with H<sub>2</sub>O or D<sub>2</sub>O as ligands. Also, a few observations were made of the C<sub>6</sub>H<sub>5</sub>D-H<sub>2</sub><sup>18</sup>O dimer. Our initial interest was in the dimers with monodeutero benzene. Prompted by the symmetric top behavior (Tables I-III) of the four dimers between the parent D<sub>6h</sub> benzene and the less symmetric water species, H<sub>2</sub>O, D<sub>2</sub>O, H<sub>2</sub><sup>18</sup>O, and HDO, we wondered whether the high effective symmetry of the dimer would survive monosubstitution on the benzene. Then, when it became apparent that transitions needed to be checked to avoid misassigning those for <sup>13</sup>C at natural abundance, the latter were also cataloged and included. In the structural analysis, the rotational constants for the dimers with monosubstituted benzene provide information about tilt of the benzene.

The assignments for the  $m=0$  states are given in Table V. The four dimers are prolate, near-symmetric tops with ( $B-C$ ) about 45 MHz for the monodeutero species and 15 MHz for the mono-<sup>13</sup>C. However,  $A$  is relatively small,  $\sim 2750$  MHz, so their asymmetry parameters  $\kappa$  are also somewhat smaller than the  $-1$  prolate limit, about  $-0.95$ .

The transitions were fitted using the basic treatment of Kivelson and Wilson<sup>14</sup> but limiting centrifugal distortion to the symmetric top terms  $D_J$  and  $D_{JK}$ .<sup>15</sup> The residues of the fits are included in Table V and the rotational constants obtained are presented in Table VI. The residues for fitting the two dimers of monodeutero benzene are reasonable, having  $\sigma=6$  kHz. Those for the mono-<sup>13</sup>C isotopomers are an order of magnitude larger, reflecting mainly the weakness of the natural abundance transitions.

Several attempts were made to identify and assign transitions of the  $m=1$  internal rotor state for these asymmetric tops, but with only limited success. The nature of the problem is shown in Fig. 2 which is a stick spectrum for the  $J=2 \rightarrow 3$  frequency range of C<sub>6</sub>H<sub>5</sub>D-H<sub>2</sub>O. The transitions assigned to the  $m=0$  state (Table V) are marked with an asterisk while some of the unmarked transitions are tentatively identified as  $m=1$ . The  $m=0$  transitions were assigned on the basis of rotational constants estimated from those found for the corresponding symmetric tops (Table III). However, the  $m=1$  transitions do not have an identifiable pattern such as that of the symmetric tops (Fig. 1) nor have they lent themselves to a computational fitting approach. For the latter we used the principal-axis method (PAM) and programs as developed by Taleb-

TABLE V. Observed and fitted rotational transition frequencies for benzene-water dimers with  $m=0$  free internal rotor, asymmetric top ground states.

Transition $J_{po} \rightarrow J'_{po}$	$C_6H_5D-H_2O$		$C_6H_5D-D_2O$		$C_5^{13}C-H_2O$		$C_5^{13}C-D_2O$	
	Obs. (MHz)	Res. (kHz)	Obs. (MHz)	Res. (kHz)	Obs. (MHz)	Res. (kHz)	Obs. (MHz)	Res. (kHz)
$0_{00} \rightarrow 1_{01}$	3 936.9925	0.1	3 774.9310	6.5	3 968.560	125	3 803.896	34
$1_{11} \rightarrow 2_{12}$	7 826.7931	-3.7	7 506.3521	-9.4	7 921.737	50	7 593.557	-19
$1_{01} \rightarrow 2_{02}$	7 871.8327	0.4	7 548.1661	-3.8	7 936.828	291	7 607.540	128
$1_{10} \rightarrow 2_{11}$	7 920.7441	13.0	7 592.8149	1.2	7 952.030	50	7 621.434	-5
$2_{12} \rightarrow 3_{13}$	11 738.7295	-1.8	11 258.3481	-6.0	11 882.279	38	11 390.045	135
$2_{02} \rightarrow 3_{03}$	11 802.3892	-1.8	11 318.0682	-0.9	11 904.011	34	11 410.228	-116
$2_{21} \rightarrow 3_{22}$	11 809.8096	2.7	11 323.3832	11.7	11 904.535	-640	11 410.687	112
$2_{20} \rightarrow 3_{21}$	11 818.0698	-12.8	11 329.7487	6.0	11 909.056	a	11 410.849	-409
$2_{11} \rightarrow 3_{12}$	11 879.5780	2.6	11 387.9937	-1.8	11 927.710	32	11 431.837	134
$3_{13} \rightarrow 4_{14}$	15 648.9954	9.0	15 008.9737	3.5	15 842.437	-17	15 186.148	449
$3_{03} \rightarrow 4_{04}$	15 726.6641	-3.4	15 083.0265	4.2	15 871.393	a	15 211.710	a
$3_{22} \rightarrow 4_{23}$	15 744.4271	-4.1	15 096.1955	-2.0	15 872.078	a	15 211.719	-626
$3_{31} \rightarrow 4_{32}$	15 748.6018	2.1	15 098.7527	7.6	15 874.112	109	15 213.093	60
$3_{30} \rightarrow 4_{31}$	15 748.9452	1.3	15 098.9544	-11.9	15 874.121	97	15 213.118	77
$3_{21} \rightarrow 4_{22}$	15 764.9571	1.4	15 112.0407	1.2	15 878.502	a	15 214.668	-355
$3_{12} \rightarrow 4_{13}$	15 836.5083	-2.6	15 181.6483	-5.0	15 903.007	-13	15 241.860	442

\*Not included in the fit. See the text.

Bendiab *et al.*<sup>16</sup> for treating internal rotation of the  $C_6H_6-SO_2$  dimer. Our lack of success with them might be because the programs treat as constant a parameter which is  $J, K$  dependent for the benzene-water dimer. In particular we found that the PAM  $m=1$  frequencies are sensitive to the orientation of the internal rotor axis with respect to the inertial frame.

An interesting regularity was observed in the  $J=0 \rightarrow 1$  frequency range of the six asymmetric top dimers studied, including the two isotopomers with  $H_2^{18}O$ . Each exhibits a symmetrical doublet, with a splitting of 0.3 to 1.3 MHz. The doublets are some 20 to 60 MHz below the  $m=0$ ,  $J=0 \rightarrow 1$  transition of that species, the displacement being close to that between the  $m=0$  and  $m=1$ ,  $J=0 \rightarrow 1$  transitions (nondoublet) of the parent symmetric top. On this basis, the doublets are assigned to the  $m=1$  state of the asymmetric tops and associated with the reduction in symmetry from sixfold to twofold by the mono- $^{13}C$  or D substitution in  $C_6H_6$ . In several of the transitions, hfs from the deuterium quadrupole interaction was observed, but it was readily distinguished from the larger doublet splitting.

These results are summarized in Table VII. It is seen that the splittings for the dimers with monodeuterobenzene are about twice those for the mono- $^{13}C$  benzene. Also, the

splittings for each monosubstituted benzene change systematically with isotopic substitution in the water. Accordingly, we attribute the splittings to perturbation of the (small) sixfold barrier in the symmetric top dimers by the monosubstitution in benzene, the small perturbation being larger for deuterium than for  $^{13}C$ . Such effects are quite common, for example, in  $CH_2DOH$  compared to  $CH_3OH$ .<sup>17</sup>

The perturbation adds a term with twofold symmetry ( $V_2$ ) to the rotational barrier, which by its symmetry splits the otherwise degenerate  $m = \pm 1$ ,  $J=0 \rightarrow 1$  transition. For small splittings, PAM calculations<sup>16</sup> show that  $v_s$  is  $2V_2$ . So the  $v_s$  values in Table VII correspond to  $V_2$  barriers of  $\sim 0.5$  MHz, which appear to be the smallest yet measured. The calculations also predict that the  $m=1$ ,  $K=0$  transitions at higher  $J$  should be similar doublets but they were not identified among the transitions observed, e.g., in Fig. 2.

### Nuclear spin states and hyperfine structure (hfs)

There are several weak hyperfine interactions in the various isotopic species of the benzene-water dimers. Thus far we have neglected them; however, resolution and anal-

TABLE VI. Rotational constants determined from the  $m=0$  transitions of the asymmetric top, benzene-water dimers.

Constant	$C_6H_5D-H_2O$	$C_6H_5D-D_2O$	$C_5^{13}CH_6-H_2O$	$C_5^{13}CH_6-D_2O$
$A$ (MHz)	2765.5(2)	2765.5(3)	2581(213)	2754(138)
$B$	1991.986(1)	1909.082(1)	1991.79(6)	1908.91(6)
$C$	1945.019(1)	1865.856(1)	1976.65(6)	1894.98(6)
$D_J$ (kHz)	3.24(3)	3.47(4)	2(2)	6(1)
$D_{JK}$	35.8(1)	44.5(1)	-2(8)	19(5)
$\sigma$ (kHz)	5.5	6.2	212	279

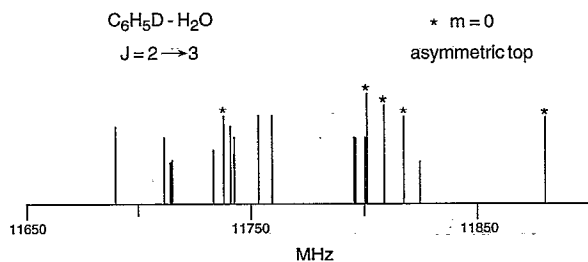


FIG. 2. Stick diagram of the spectral region for the  $J=2 \rightarrow 3$  transitions of the  $C_6H_5D-H_2O$  dimer. The lines marked with an asterisk are assigned to the  $m=0$  internal rotation state and fitted as an asymmetric top (Table V). Some of the unassigned lines are from the  $m=1$  internal rotor state. Not shown are the more than 30 relatively weak lines found between 11 690 and 11 880 MHz, and a cluster of 14 stronger lines between 11 670 and 11 690 MHz.

ysis of the hfs they produce can augment our understanding of the dimers. The largest hf interaction is the deuterium nuclear quadrupole coupling  $\chi_0(D)$  in HDO and  $D_2O$ , the values for which have been cited to be 315 and 330 kHz, respectively, in the free monomer.<sup>18,19</sup> The next largest is  $\chi_0(D)$  in monodeutero benzene for which 223(12) kHz has been reported.<sup>20</sup>

The next smaller hf interaction is the proton-proton magnetic dipole-dipole interaction where

$$D_0(H-H) = -2g_H^2\mu_N^2/r^3, \quad (2)$$

in which  $g_H$  is the magnetogyric ratio of the proton,  $\mu_N$  is the nuclear magneton, and  $r$  is the particular H-H distance. For  $H_2O$ , where  $r(H-H)$  is<sup>21</sup> 1.518 Å, Eq. (2) gives  $D_0(H-H)$  to be -69.1 kHz. The smaller  $g$ -value of deuterium reduces  $D_0(H-D)$  to -10 kHz in HDO, which we neglect. Similarly the  $D_0(H-H)$  of ortho protons in benzene is predicted to be -15.6 kHz. This and the spin-rotation interaction in the  $H_2O$  are large enough to cause sometimes discernible effects,<sup>19</sup> which we ignore.

Two aspects of the hfs are useful in the present context. It is a guide to the nuclear spin statistics and symmetry of the various isotopomers and internal rotor states. Also, its magnitude is dependent on the internal dynamics. The spectra observed are  $a$ -dipole transitions with the  $a$  axis

TABLE VII. The  $m=1$  doublets for asymmetric tops: A comparison of the  $m=0$  and  $m=1$ ,  $J=0 \rightarrow 1$  frequencies (MHz) observed for symmetric top ( $C_6H_6$ ) and asymmetric top ( $C_6H_5D$  and  $C_5^{13}CH_6$ ) benzene-water dimers.

Dimer	$\nu(m=0)$	$\nu(m=1)$	$\Delta\nu^a$	$\nu_s^b$
$C_6H_6-H_2^{18}O$	3767.411	3744.512	22.899	
$-H_2O$	3989.536	3963.295	26.241	
$-D_2O$	3824.012	3765.534	58.478	
$C_5^{13}CH_6-H_2^{18}O$	3747.696	3725.295	3724.948	0.347
$-H_2O$	3968.560	3942.900	3942.482	25.869
$-D_2O$	3803.896	3745.762	3745.123	58.454
$C_6H_5D-H_2^{18}O$	3719.545	3698.140	3697.373	21.789
$-H_2O$	3936.993	3912.508	3911.556	24.961
$-D_2O$	3774.931	3720.435	3719.016	55.206

<sup>a</sup> $\Delta\nu = \nu(m=0) - \nu(m=1)$  (average) for asymmetric tops.

<sup>b</sup> $\nu_s$  is the splitting of the doublet which also is  $2V_2$ .

either the principal symmetry axis of the dimer or close to it. Therefore the coupling constants determined are projections of  $D_0$  or  $\chi_0$  onto the  $a$  axis, averaged over the dynamics. This is described by

$$D_{aa}(H-H) = \frac{1}{2}D_0(H-H) \langle 3 \cos^2 \theta - 1 \rangle, \quad (3)$$

where  $\theta$  is the angle between the H-H axis and the  $a$  axis of the dimer. A similar expression applies to  $\chi_0(D)$  if it has cylindrical symmetry about the O-D bond. As an example, we consider the ortho pairs of protons in the benzene of the benzene-water dimer. The H-H vectors for them are perpendicular or near-perpendicular ( $\theta=90^\circ$ ) to the  $a$ -axis. Thereby their  $D_{aa}(H-H)$  value is reduced to  $-D_0/2$  or about 7.8 kHz, supporting their neglect.

### $C_6H_6-H_2O$ , $-H_2^{18}O$ , and $-D_2O$

We turn now to the symmetry and spin statistics of the  $C_6H_6-H_2O(H_2^{18}O)$  and  $C_6H_6-D_2O$  dimers, which have symmetric top transitions in the  $m=0$  and  $m=1$  states. If the dimers have the  $C_2$  axis of the  $H_2O$  coaxial with the  $C_6$  axis of the benzene, and they are free or nearly free to internally rotate, their permutation-inversion properties are those of the  $G_{24}$  molecular symmetry group, as found by Gotch and Zwier.<sup>2</sup> In  $C_6H_6-H_2O$  (and  $-H_2^{18}O$ ) this predicts that the nuclear spin state of the water's protons are antisymmetric ( $I_H=0$ ) to exchange of the protons in the  $m=0$  ground state rotational levels, and symmetric ( $I_H=1$ ) in the  $m=1$  levels. In  $C_6H_6-D_2O$  the reverse applies, symmetric spin states ( $I_D=0,2$ ) are required for  $m=0$  and antisymmetric ( $I_D=1$ ) for  $m=1$ . This behavior is similar to that found for the argon-water dimer.<sup>13,19</sup>

The relative statistical weights of the  $I_H=0$  and  $I_H=1$  states of  $H_2O$  are 1 and 3, respectively. Therefore, the intensities of corresponding  $m=0$  and  $m=1$  transitions of  $C_6H_6-H_2O$  should be approximately 1 to 3. Similarly, the statistical weights of  $I_D=0, 2$  and  $I_D=1$  in  $D_2O$  are 6 and 3, so the relative intensities of corresponding  $m=0$  and  $m=1$  transitions for  $C_6H_6-D_2O$  should be approximately 2 to 1. The intensities observed are generally as predicted.

The various hf interactions produce resolved splittings primarily in the  $J=0 \rightarrow 1$  and  $1 \rightarrow 2$  ( $K=0,1$ ) transitions and of necessity we limit our considerations to them. Such results for the small  $D_0(H-H)$  coupling in the  $C_6H_6-H_2O$  dimer are summarized in Table VIII. For the  $m=0$  state these transitions are sharp singlets, as predicted for the  $H_2O$  protons in an antisymmetric  $I_H=0$  spin state. For the  $m=1$  state, the protons are predicted to be in the symmetric  $I_H=1$  spin state and all transitions should exhibit the corresponding hfs, but in fact, only the  $K = \pm 1$  transitions were found to have hfs while the  $K=0$  transitions are sharp singlets as for the  $m=0$  state. The observed hfs includes two strong central components; it was fitted as described elsewhere,<sup>9,19</sup> using the basis set  $I_H+J=F$ . The results are given in Table VIII for the best resolved transition ( $J=1 \rightarrow 2$ ,  $K=+1$ ), including the values fitted for  $D_{gg}$ . The latter place the H-H axis of the  $H_2O$  perpendicular to the sixfold axis of the dimer.

The case of  $C_6H_6-D_2O$  is more difficult and less persuasive because both the  $m=0$  and  $m=1$  states have hfs

TABLE VIII. The magnetic dipole hfs observed in the  $J=0 \rightarrow 1$  and  $J=1 \rightarrow 2$  transitions for the  $m=0$  and  $m=1$  states of  $C_6H_6-H_2O$ ,<sup>a</sup> and the symmetry of the proton spin functions  $\psi_n$  in the  $H_2O$ .<sup>b</sup>

$J,K$	hfs	MHz	$\psi_n$ (obs)	$\psi_n$ (pred)
$m=0$ state				
$J=0 \rightarrow 1, K=0$	Singlet	3989.5344	$a, I_H=0$	$a, I_H=0$
$J=1 \rightarrow 2, K=1$	Singlet	7978.8365	$a$	$a$
$J=1 \rightarrow 2, K=0$	Singlet	7978.9876	$a$	$a$
$m=1$ state				
$J=0 \rightarrow 1, K=0$	Singlet	3963.2973	$a, I_H=0$	$s, I_H=1$
$J=1 \rightarrow 2, K=-1$	"Doublet"	7919.7166	$s, I_H=1$	$s$
		9.7378		
$J=1 \rightarrow 2, K=0$	Singlet	7926.9689	$a, I_H=0$	$s$
$J=1 \rightarrow 2, K=+1$	"Doublet"	7981.4211 <sup>c</sup>	$s, I_H=1$	$s$
		1.4350		

Fit of hfs for the  $J=1 \rightarrow 2, K=+1$  ( $1_{10} \rightarrow 2_{11}$ ) transition of the  $m=1$  state.

$F \rightarrow F'$	Obs. (MHz)	Res. (kHz)	Parameters fitted
1 $\rightarrow$ 1	7981.4043	-1.1	
1 $\rightarrow$ 2	1.4211	0.3	$D_{bb}$ -72(4) kHz
2 $\rightarrow$ 3	1.4350	2.6	$D_{cc}$ 31(5)
2 $\rightarrow$ 2	1.4410	-1.2	
0 $\rightarrow$ 1	1.4585	-0.6	

<sup>a</sup>Completely equivalent hfs was found for the  $C_6H_6-H_2^{18}O$  species.

<sup>b</sup>The statistical weights of the  $a/s$  spin functions are 1/3.

<sup>c</sup>This is a displaced transition as shown in Fig. 1. Details of the hfs are given in the bottom part of this table.

which is more complex than for the dimer with  $H_2O$ . The results with  $D_2O$  are very similar to those with  $H_2O$  but differ as shown in Table IX. For  $m=0$ , the deuterium spin states are all found to be symmetric ( $I_D=0,2$ ) as predicted. But for  $m=1$ , the  $K=0$  transitions have the predicted antisymmetric deuterium spin states ( $I_D=1$ ) while the hfs of the  $K=\pm 1$  transitions seems more attributable to symmetric deuterium spin states, counter to predictions.

TABLE IX. Deuterium quadrupole hfs observed in the  $J=0 \rightarrow 1$  and  $J=1 \rightarrow 2$  transitions for the  $m=0$  and  $m=1$  states of  $C_6H_6-D_2O$ , and the symmetry of the deuterium spin functions  $\psi_n$  in the  $D_2O$ .

$J,K$	hfs	MHz	$\psi_n$ (obs)	$\psi_n$ (pred)
$m=0$ state				
$J=0 \rightarrow 1, K=0^a$	"Triplet"	3823.9816	$s, I_D=0,2$	$s, I_D=0,2$
		4.0063		
		4.0275		
$J=1 \rightarrow 2, K=1$	"Quartet"	7647.7535	$s, I_D=0,2$	$s$
$J=1 \rightarrow 2, K=0$	"Singlet"	7.9331	$s, I_D=0,2$	$s$
$m=1$ state				
$J=0 \rightarrow 1, K=0^a$	Triplet	3765.5209	$a, I_D=1$	$a, I_D=1$
		5.5349		
		5.5555		
$J=1 \rightarrow 2, K=-1$	Multiplet	7511.852	$s, I_D=0,2$	$a$
$J=1 \rightarrow 2, K=0$	"Singlet"	7533.679	$a, I_D=1$	$a$
$J=1 \rightarrow 2, K=+1$	Multiplet	7656.735	$s, I_D=0,2$	$a$

<sup>a</sup>The hfs for the  $J=0 \rightarrow 1, m=0$  and  $m=1$  transitions corresponds to  $\chi_{aa}(D) = -131$  and  $-46$  kHz, respectively, for which Eq. (3) gives  $\theta = 75^\circ$  and  $61^\circ$ .

TABLE X. Observed and fitted deuterium hfs in the  $J=0 \rightarrow 1, K=0$  transitions of  $C_6H_6-HDO$  and  $C_6H_5D-H_2^{18}O$ .

$F \rightarrow F'$	$C_6H_6-HDO$		$C_6H_5D-H_2^{18}O$	
	Obs. (MHz)	Res. (kHz)	Obs. (MHz)	Res. (kHz)
1 $\rightarrow$ 0	3912.5090	-0.2	3719.5962	0
1 $\rightarrow$ 2	2.5853	0.4	9.5503	0
1 $\rightarrow$ 1	2.6352	-0.2	9.5198	0
Parameters determined				
Line center, MHz	3912.5933(3)		3719.5452	
$\chi_{aa}(D)$ , kHz	168.3(9)		-101.9(1)	
$\theta$ , deg	33.99 <sup>a</sup>			

<sup>a</sup>If  $\theta$  is assumed to be  $90^\circ$ ,  $\chi_0(D)$  is determined to be 203.8 kHz.

The hfs could be analyzed in some detail for the  $J=0 \rightarrow 1, K=0$  transitions of both the  $m=0$  and  $m=1$  states of  $C_6H_6-D_2O$ . In these transitions the hfs calculated for antisymmetric  $I_D=1$  spins is a triplet with a spacing ratio of 0.67. That for the symmetric  $I_D=0, 2$  spins is also a "triplet," but made up of a singlet from  $I_D=0$  and a triplet from  $I_D=2$ . The singlet is unresolved from the center component of the triplet, giving an approximate spacing ratio of 1.33. Comparison of these predictions with the hfs reported in Table IX assigns the  $m=0, J=0 \rightarrow 1$  transition unambiguously to the symmetric  $I_D=0, 2$  spin state and the  $m=1$  to the antisymmetric  $I_D=1$  state. The 45.9 kHz between the outer components<sup>9</sup> of the  $m=0$  transition is  $0.35 \chi_{aa}(D)$  which gives  $\chi_{aa}(D) = -131$  kHz, the sign determined by the asymmetry in splittings of the triplet. In Eq. (3) this leads to a value of  $75^\circ$  for the approximate average angle between the OD bonds and the  $a$  axis. The  $m=1$  state has the usual  $J=0 \rightarrow 1$  triplet hfs from a spin-1 nucleus. The 34.6 kHz separation of its outer components leads to value of  $-46.1$  kHz for  $\chi_{aa}(D)$ , the sign established by asymmetries in intensities and splittings. This corresponds to a  $\theta$  of  $61^\circ$  via Eq. (3).

A similar approach was used to assign the deuterium spin states in  $C_6H_6-D_2O$  for the  $J=1 \rightarrow 2$  transitions, giving the results in Table IX. Here the differences in hfs for symmetric versus antisymmetric spin states are appreciable for the "singlet"  $K=0$  transitions, but less apparent for the more complex  $K=\pm 1$  transitions.

### $C_6H_6-HDO$

For this dimer the  $m=1$  state relaxes to the  $m=0$  in the jet expansion because the process is not spin forbidden. Because of this our measurements are limited to the  $m=0$  state. The  $\chi_0(D)$  is relatively large (315 kHz) and hfs from it was resolved in 6 of the 10  $\Delta J=1, \Delta K=0$  symmetric top transitions observed. That for  $J=0 \rightarrow 1, K=0$  and the results of its fit are given in Table X. The triplet structure is characteristics of a  $J=0 \rightarrow 1$  transition for an  $I=1$  nuclear species. When fitted it yields a value for  $\chi_{aa}(D)$  of 168.3 kHz. This result was employed to predict the hfs expected for a symmetric top in the other nine  $J,K$  transitions (four singlets, three doublets, and two triplets). The

prediction has several minor discrepancies, probably because  $\chi_{gg}$  is not quite axially symmetric, as assumed. Nonetheless, it should be a good approximation to use Eq. (3) to indicate the average orientation of the O-D bond in the dimer. The 168.3 kHz found for  $\chi_{aa}(\text{D})$  corresponds to  $\theta=34^\circ$ , which indicates that the deuterium is preferentially hydrogen bonded to the benzene.

### $\text{C}_6\text{H}_5\text{D}-\text{H}_2\text{O}$ and $-\text{H}_2^{18}\text{O}$

The hfs of the monodeutero benzene in these species offers an opportunity to determine a value of  $\chi_0(\text{D})$  in benzene. The  $J=0 \rightarrow 1$  transitions for their  $m=0$  and  $m=1$  states, listed in Table VII, all exhibit the triplet hfs expected for  $I=1$  quadrupolar nuclei, with low and high frequency splittings of 30 and 45 kHz. A typical set of measurements, that for  $\text{C}_6\text{H}_5\text{D}-\text{H}_2^{18}\text{O}$ , is included in Table X with the results of its fit. In this case the C-D axis is perpendicular to the  $a$  axis ( $\theta=90^\circ$ ) except for vibrational tilt of the benzene. Neglecting the tilt, we find via Eq. (3) a lower-bound value of 205 kHz for  $\chi_0(\text{D})$ . A value of 223(12) kHz was found<sup>20</sup> from hfs observed in the  $0_{00} \rightarrow 1_{01}$  pure rotational transition of  $\text{C}_6\text{H}_5\text{D}$ .

Transitions of the dimers exhibit evidence only of the deuterium quadrupole interactions. The H-H dipole interactions could produce additional resolvable splittings but this was not the case. Trial calculations with both interactions show that  $D_{aa}(\text{H-H})$  in an  $I_{\text{H}}=1$  spin state should split the  $F=1 \rightarrow 1$   $\chi_{aa}(\text{D})$  hf component into a resolvable triplet. Lacking that,  $D_{aa}(\text{H-H})$  should perturb the ratio of the splittings from its usual 2/3 value. The absence of such effects implies that the two protons are in the singlet  $I_{\text{H}}=0$  spin state for the  $J=0 \rightarrow 1$  transitions in both  $m=0$  and  $m=1$  states.

### Structural analysis

The results and analyses given above have several implications of a structural nature which we consider here. Our observations are consistent with and augment the basic structural model presented by Gotch and Zwier<sup>2</sup> and Blake's group<sup>5</sup> for the benzene-water dimer. In it the water on average is attached symmetrically, hydrogens first, to one face of the benzene ring, with the water c.m. (center of mass) on the benzene sixfold axis. The PES at the water leaves it free or nearly free to rotate internally ( $V_6 \lesssim 2 \text{ cm}^{-1}$ ), as suggested by Dykstra's MMC calculations.<sup>3</sup>

A striking experimental feature of the dimers is that all isotopomers ( $\text{H}_2\text{O}$ , HDO,  $\text{D}_2\text{O}$ ,  $\text{H}_2^{18}\text{O}$ ) with the parent  $\text{C}_{6h}$  benzene ( $\text{C}_6\text{H}_6$ ) are symmetric tops in both  $m=0$  and  $m=1$  states (Table III) while those with a monosubstituted benzene are asymmetric tops (Table VI and Fig. 2). A question similar to this was reviewed by Cox<sup>10</sup> who considered several covalent molecules, such as  $\text{CH}_3\text{NO}_2$  and  $\text{CF}_3\text{NO}_2$ , with two coaxial symmetric rotors and a sixfold barrier. He pointed out that in such cases the nature of the rotational spectrum depends on the value of the reduced barrier height,  $s=V_6/9F$  where  $F=A(\text{top})+A(\text{frame})$  is the reduced rotational constant for the top and framework. For a light top and low barrier the rotational

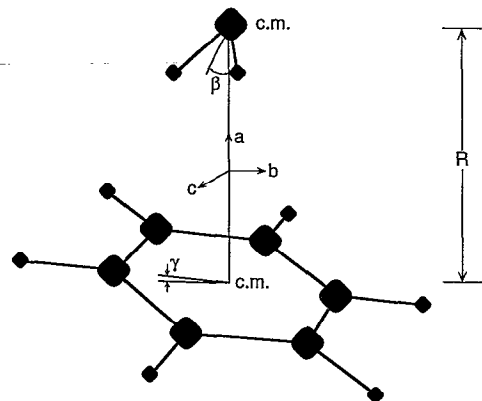


FIG. 3. Molecular geometry of the  $m=0$  and  $m=1$  states of the benzene-water dimer. Virtually free internal rotation of the water makes the dimer a symmetric top. Three structural parameters are determined for the  $m=0$  state: the c.m. to c.m. distance  $R$  and the average angular displacements  $\beta$  and  $\gamma$  of the  $\text{H}_2\text{O}$   $C_2$  axis and the  $\text{C}_6\text{H}_6$   $C_6$  axis from the  $a$  axis.

spectrum of the  $m=0$  state is that of the semirigid frame, i.e., rotation of the top ( $I_\alpha$ ) does not contribute to the overall  $A$  rotational constant, only to  $B$  and  $C$ .

In  $\text{C}_6\text{H}_6-\text{H}_2\text{O}$  the frame consists of benzene and the on-axis oxygen. One rotor is the benzene rotating about its sixfold axis ( $c$ ) while the other is the water rotating about an undefined axis (nominally its  $b$  axis) at an unknown orientation with respect to the frame. For the dimer then,  $A$  (frame) is  $C$  (benzene) = 2.84 GHz (Ref. 22) and  $A$  (top) is nominally  $B$  ( $\text{H}_2\text{O}$ ) = 435.35 GHz.<sup>23</sup> Therefore with a  $V_6$  of  $1 \text{ cm}^{-1}$ , this gives a very low effective barrier height  $s$  of 0.0076 and a symmetric top spectrum. Moreover,  $A$  (frame) is much smaller (150-fold) than  $A$  (top). This then accounts for the asymmetric top spectra of the dimers with the monosubstituted benzenes and is the reason why  $\text{D}_2\text{O}$  substitution does not affect  $A$  in  $\text{C}_6\text{H}_5\text{D}-\text{H}_2\text{O}$  (Table VI). It also explains our observation of only one structural isomer of the dimers with monosubstituted benzene. The semirigid  $\text{C}_6\text{H}_5\text{D}-\text{O}$  and  $\text{C}_5^{13}\text{CH}_6-\text{O}$  frames are asymmetric tops and the dimers give the corresponding rotational spectra (Table V and Fig. 2). Similarly, the dimers with a  $\text{C}_{6v}$  symmetric,  $\text{C}_6\text{H}_6-\text{O}$  semirigid frame have symmetric top rotational spectra for the different water isotopomers, including HDO which does not have  $\text{C}_{2v}$  symmetry.

This insensitivity of the spectrum type to isotopic substitution and asymmetry of the water is a consequence of its relatively modest and isotropic binding to the benzene. Thereby the  $m=0$  and  $m=1$  states of the dimers correlate strongly with the  $0_{00}$  and  $1_{11}$  (or other  $J=1$ ) levels of free water, and the atomic positions get axially averaged. A similar case is the  $\text{Ar}-\text{H}_2\text{O}$  dimer which has been studied extensively.<sup>13,19,24,25</sup> As in it, the isotropic PES and internal rotation of  $\text{C}_6\text{H}_6-\text{H}_2\text{O}$  make its structure more than usually fuzzy. So we limited our analyses to the  $m=0$  data and assumed an axially symmetric, averaged structure for the dimer. The structural parameters considered are the orientation of the  $\text{H}_2\text{O}$  with respect to the benzene ring, the c.m.

( $C_6H_6$ ) to c.m. ( $H_2O$ ) distance  $R$ , the angle  $\beta$  between the  $H_2O$   $C_2$  axis and the equilibrium sixfold axis of the benzene, and the average angular tilt  $\gamma$  of benzene from having its plane perpendicular to the  $a$  axis (Fig. 3).

In the dimer, the water is oriented with the oxygen away from the benzene ring. This is seen most directly by the  $m=0$   $B_0$ 's in Table III which decrease progressively with isotopic substitution of the water in the sequence  $H_2O$ , HDO,  $D_2O$ , and  $H_2^{18}O$ . The mass increase in the parent  $C_6H_6-H_2O$  upon  $D_2O$  substitution is virtually identical with  $H_2^{18}O$  substitution. But  $B_0$  decreases for  $^{18}O$  by 111 MHz compared with 83 MHz for  $D_2$ , clearly placing the O well outside the H's.

We develop a more quantitative picture by applying an isotopic substitution analysis using  $C_6H_6-H_2O$  as the parent species.<sup>9</sup> The position of the oxygen along the  $a$  axis,  $a_O$ , is determined readily from the  $B$  rotational constant for  $C_6H_6-H_2^{18}O$  as  $\Delta I_b = \mu_s a_O^2$ . Here  $\Delta I_b$  is the change in the parent's moment of inertia upon  $^{18}O$  substitution,  $\mu_s$  is the reduced mass  $M\Delta m/(M+\Delta m)$  for the substitution, and  $a_O$  is the distance of the oxygen along the  $a$  axis from the dimer c.m. (parent). This gives a value of 2.7581 Å for  $a_O$ . The hydrogens are off-axis but an upper bound  $a_{H'}$  can be placed upon  $a_H$  by treating them as jointly on axis in the deuterated species  $C_6H_6-D_2O$ . The result is  $a_{H'} < 2.3586$  Å, showing that the oxygen is well outside the hydrogens of the water, but the difference of 0.40 Å between  $a_O$  and  $a_{H'}$  is appreciably smaller than the altitude (0.5953 Å) of free  $H_2O$ ,<sup>20</sup> suggesting that the  $H_2O$   $C_{2v}$  axis is not really effectively coincident with the sixfold axis.

The orientation of the  $H_2O$  can be refined by considering the symmetric top behavior ( $I_b = I_c$ ) of the dimers and the equivalence of the hydrogens in them as shown by their hfs. This encourages us to treat the  $H_2O$  and  $D_2O$  as rotors with threefold symmetry and the substitution of  $D_2O$  for  $H_2O$  as a multiple off-axis substitution<sup>9</sup> of  $\Delta m' = (2/3)(m_D - m_H) = (2/3)\Delta m$ . This gives  $\Delta I_b$  as the following function of both  $a_H$  and  $b_H$ :

$$\Delta I_b = \Delta m b_H^2 + [2\Delta m M / (M + 2\Delta m)] a_H^2, \quad (4)$$

where  $b_H^2 + \Delta a_H^2 = r(OH)^2$  and  $\Delta a_H = a_O - a_H$ . These relations yield values of 2.2815 Å for  $a_H$  and 0.8476 Å for  $b_H$ , from which  $\Delta a_H$  is 0.4766 Å. The latter is the projection of the  $H_2O$  altitude onto the  $a$  axis, giving a projection angle of 37°, as the on average angle  $\beta$  between the two axes.

A substitution analysis was made of the three rotational constants determined for each of the asymmetric top dimers with  $H_2O$  (Table VI). With  $C_6H_6-H_2O$  as the parent, the deuterium and  $^{13}C$  monosubstitution enable one<sup>9</sup> to determine both  $a_s$  and  $b_s$  for the substituent. However, the benzene c.m. is close to the dimer c.m. ( $\sim 0.6$  Å) so the apparent values found for  $a_C$  and  $a_H$  are unreliable. The analysis does give reasonable values for  $b_C$  and  $b_H$  of 1.407 and 2.489 Å. These are somewhat larger than the values of 1.396 and 2.479 Å reported for free benzene.<sup>26</sup> This implies little or no tilt ( $\gamma \sim 0^\circ$ ) of the benzene inasmuch as the tilt would foreshorten both  $b_C$  and  $b_H$ .

A value can be found for  $R$  by applying the first moment condition to the position of the  $H_2O$  c.m. on the  $a$

axis. The substitution analysis for  $C_6H_6-H_2^{18}O$  gave us  $a_O = 2.7581$  Å. It is reduced to 2.7049 Å for the  $H_2O$  c.m. by projection of the O to c.m. distance (0.0666 Å) onto the  $a$  axis. This gives  $a = -0.6242$  Å for the  $C_6H_6$  c.m. and  $R = 3.3291$  for the  $C_6H_6-H_2O$  dimer. The uncertainty in this result comes mainly from the dynamic state of the  $H_2O$  and questions in how best to deal with it. The problems persist in a pseudodiatomic approach<sup>27</sup> based on the moments of inertia for the monomers and the dimer.<sup>5</sup>

A substitution analysis with  $C_6H_6-D_2O$  as parent gives results compatible with those from  $C_6H_6-H_2O$ .

## DISCUSSION

The overall picture emerging from this analysis of the rotational spectrum for the benzene-water dimer is basically that of Zwier,<sup>2</sup> Dykstra,<sup>3</sup> and Blake.<sup>5</sup> The  $H_2O$  is hydrogen bonded to one face of the benzene, at an unremarkable c.m. to c.m. distance of 3.329 Å in  $C_6H_6-H_2O$ . The minimum in the potential energy surface is relatively shallow and isotropic at the  $H_2O$ , not only leaving it free to rotate readily but also allowing changes in the rotational axis.

As yet a number has not been placed on  $V_6$ , the sixfold barrier to internal rotation of the  $H_2O$ . Symmetry conditions require observation of  $m=3$  transitions for this purpose.<sup>16</sup> This seems unlikely in nozzle expansion experiments because of their low temperatures ( $\sim 3$  K) and the large rotational constants of  $H_2O$  ( $\sim 500$  GHz) which cause only its lowest rotational states to be populated. In fact we have searched unsuccessfully for  $m=2$  transitions. However, our finding that  $V_2$  is only about half a MHz in the dimers with monosubstituted benzenes offers indirect evidence for a very small  $V_6$ . In  $CH_2D-OH$ ,  $V_1$ , and  $V_3$  are 12 and 375  $cm^{-1}$ , respectively.<sup>17</sup>

The weak coupling of the  $H_2O$  to the inertial frame, and its large rotational excitation energy, make the rotational states of  $H_2O$  in the dimer essentially those of the free monomer. Nonetheless the potential energy surface orients the  $H_2O$  and its axis of rotation with respect to the inertial frame. Both the substitution and the hfs analyses show that the  $C_2$  axis of the  $H_2O$  is at a significant on average angle ( $\beta = 35^\circ$ ) to the sixfold axis. Also, it seems likely that the internal rotation of the water is about its  $C_2$  axis. Moreover, analysis of the hfs in  $C_6H_6-HDO$  shows the D to be preferentially bonded to the benzene.

The most direct information about the rotational state of the water is obtained in principle from the hfs analyses for  $C_6H_6-H_2O$  and  $-D_2O$  which determine the symmetry of the nuclear spin functions  $\psi_n$  associated with the various rotational transitions of the dimer. Tables VIII and IX compare our experimental results for  $\psi_n$  with the predictions of Gotch and Zwier<sup>2</sup> for a dimer in which the  $b$  axis of the freely rotating water molecule is coaxial with the sixfold axis of benzene. The spin functions determined for the  $m=0$  transitions agree with the predictions of this model but those for the  $m=1$  transitions do not.

The differences for the  $C_6H_6-H_2O$  dimer are the simplest and most persuasive (Table VIII). All of its  $m=1$  transitions are predicted to have antisymmetric  $I_H = 1$  trip-

let hfs. However, the  $m=1, J=0 \rightarrow 1$  and  $1 \rightarrow 2, K=0$  transitions are found to be sharp singlets. This behavior could be attributed either to a triplet state with the H-H vector accidentally at the magic angle to the  $a$  axis [ $\cos^2 \theta = 1/3$  in Eq. (3)], or to a true singlet state. Several factors discourage the magic angle interpretation including the substitution analysis and the relative intensities of the various  $m=1$  transitions. Also, one would expect  $\text{H}_2^{18}\text{O}$  substitution to affect  $\theta$ , but the linewidths of the  $K=0$  transitions for  $\text{C}_6\text{H}_6\text{-H}_2^{18}\text{O}$  are the same for  $\text{C}_6\text{H}_6\text{-H}_2\text{O}$ . Therefore, we accept the singlet transitions as from  $I_{\text{H}}=0$  spin states and turn to the model in which the rotational state of the water in the dimer is described by the (perturbed) rotational wave functions  $\phi_r$  for free  $\text{H}_2\text{O}(\text{D}_2\text{O})$ .

In this event, for the  $m=0$  transitions we assign  $0_{00}$  as  $\phi_r$ . Moreover, the parity of  $\phi_r \psi_n$  must be negative (positive) for the interchange of the two protons (deuterium nuclei). The parity of  $0_{00}=\phi_r$  is positive,<sup>28</sup> requiring that of  $\psi_n$  to be  $- (+)$  for  $\text{H}_2\text{O}(\text{D}_2\text{O})$ . This agrees with the experimental results in Tables VIII and IX for  $m=0$ . The  $m=1$  transitions, however, are more complex and give rotational assignments differing for  $\text{H}_2\text{O}$  and  $\text{D}_2\text{O}$ .

For  $\text{H}_2\text{O}$ , the  $m=1, K=0$  transitions have a  $\psi_n$  with  $-$  parity, requiring that  $\phi_r$  be  $+$ . But the  $K=\pm 1$  transitions are found to have a  $+\psi_n$  and require a  $-\phi_r$ , pointing to different  $m=1$  rotational states for the  $\text{H}_2\text{O}$ . The lowest excited rotational states of the  $\text{H}_2\text{O}$  are described by the three  $J=1$  wave functions, of which  $1_{01}(B+C)$  and  $1_{10}(A+B)$  are  $-$  and  $1_{11}(A+C)$  is  $+$ .<sup>28</sup> For  $\phi_r$  we need one each  $+$  and  $-$ ; of the two  $-$  possible, we take  $1_{01}$  rather than  $1_{10}$  because it is lower in energy. The final  $\text{H}_2\text{O}$  assignments are  $K=0, 1_{11}$  and  $K=\pm 1, 1_{01}$ . For  $\text{D}_2\text{O}$  the less persuasive analysis of the  $J=1 \rightarrow 2, K=\pm 1, m=1$  hfs enables us to assign  $\phi_r$  for it in the same manner. However, the assignments are reversed, being  $1_{01}$  for  $K=0$ , and  $1_{11}$  for  $K=\pm 1$ .

The existence of relatively unperturbed rotational states for monomers in dimers has been reported previously. The most notable example is probably  $\text{Ar-H}_2\text{O}$  which has two internal rotation states corresponding to  $0_{00}$  and  $1_{01}$  of free water.<sup>13,19,24,25</sup> However, the apparent complexity of the rotational states found for water in benzene seems to be something new requiring further study. It is perhaps attributable to coupling between rotation of the water and rotation of the inertial frame, which makes the rotational axis of the water change with  $J, K$  of the dimer.

Perturbations of this nature might account for the large rms deviation of  $\sim 1$  MHz and the negative term in  $D_{Jjm}$  in fitting the  $m=1$  transitions (Table III). Also, the large differences between the rotational constants for the  $m=1$  transitions of the dimers with  $\text{H}_2\text{O}$  and  $\text{D}_2\text{O}$  could be associated with the difference in their assigned rotational states. In particular, attention is called to  $D_{Jm}$  which is 29.7 MHz for  $\text{C}_6\text{H}_6\text{-D}_2\text{O}$  but only 13.1 and 11.4 MHz in  $\text{C}_6\text{H}_6\text{-H}_2\text{O}$  and  $\text{-H}_2^{18}\text{O}$ . Displacement of the  $m=1, K=+J$  components (Fig. 1 and Table IV) also begs for attention.

A final question is raised by the observation of nuclear spin functions of the same symmetry in both the  $m=0$  and

$m=1$  states. This was not only the case for the  $\text{C}_6\text{H}_6\text{-H}_2\text{O}$  and  $\text{-D}_2\text{O}$  dimers (Tables VIII and IX) but also for the  $\text{C}_6\text{H}_5\text{D-H}_2\text{O}$  and  $\text{-H}_2^{18}\text{O}$  dimers. One might expect this to provide a pathway for the otherwise spin-forbidden relaxation from some of the  $m=1$  levels to the  $m=0$  state at the low temperatures of the jet expansion. However, the  $K=0$  levels of the  $m=1$  state which might relax this way are the most intense lines of the dimers (Fig. 1).

## ACKNOWLEDGMENTS

We thank G. A. Blake and his group, especially Sakae Suzuki, for challenging us with the complexities of the benzene/water system.<sup>5</sup> Our understanding and analysis of its excited internal rotor states were aided significantly by A. Taleb-Bendiab of the Kuczkowski group, who shared with us their computer program for treating internal rotation of benzene-containing dimers.<sup>16</sup> Augspurger, Dykstra, and Zwier<sup>3</sup> provided a preprint of their study of the benzene-water interaction potential and amplified it in several helpful discussions. This material is based upon work supported by the National Science Foundation under Grant No. CHE 91-17199. In addition, acknowledgment is made to the donors of the Petroleum Research Fund, administered by the American Chemical Society, for partial support of this research.

<sup>1</sup>W. Klemperer, *Science* **257**, 887 (1992).

<sup>2</sup>A. J. Gotch and T. S. Zwier, *J. Chem. Phys.* **96**, 3388 (1992).

<sup>3</sup>J. D. Augspurger, C. E. Dykstra, and T. S. Zwier, *J. Phys. Chem.* **96**, 7252 (1992).

<sup>4</sup>G. T. Fraser, *Int. Revs. Phys. Chem.* **10**, 189 (1991).

<sup>5</sup>S. Suzuki, P. G. Green, R. E. Bumgarner, S. Dasgupta, W. A. Goddard III, and G. A. Blake, *Science* **257**, 942 (1992).

<sup>6</sup>E. Arunan and H. S. Gutowsky, *J. Chem. Phys.* **98**, 4294 (1993).

<sup>7</sup>W. H. Kirchhoff and D. R. Lide, Jr., *J. Chem. Phys.* **43**, 2203 (1965).

<sup>8</sup>G. T. Fraser, F. J. Lovas, R. D. Suenram, D. D. Nelson, Jr., and W. Klemperer, *J. Chem. Phys.* **84**, 5983 (1986).

<sup>9</sup>W. Gordy and R. L. Cook, *Microwave Molecular Spectra* (Wiley, New York, 1984).

<sup>10</sup>A. P. Cox, *J. Mol. Struct.* **97**, 61 (1983).

<sup>11</sup>T. J. Balle and W. H. Flygare, *Rev. Sci. Instrum.* **53**, 33 (1981); C. Chuang, C. J. Hawley, T. Emilsson, and H. S. Gutowsky, *ibid.* **61**, 1629 (1990).

<sup>12</sup>T. Emilsson, T. C. Germann, and H. S. Gutowsky, *J. Chem. Phys.* **96**, 8830 (1992).

<sup>13</sup>G. T. Fraser, F. J. Lovas, R. D. Suenram, and K. Matsumura, *J. Mol. Spectrosc.* **144**, 97 (1990).

<sup>14</sup>D. Kivelson and E. B. Wilson, Jr., *J. Chem. Phys.* **20**, 1575 (1952).

<sup>15</sup>A. C. Legon, P. D. Aldrich, and W. H. Flygare, *J. Chem. Phys.* **75**, 625 (1981).

<sup>16</sup>A. Taleb-Bendiab, K. W. Hillig II, and R. L. Kuczkowski, *J. Chem. Phys.* **97**, 2996 (1992).

<sup>17</sup>R. C. Quade and R. D. Suenram, *J. Chem. Phys.* **73**, 1127 (1980).

<sup>18</sup>D. Yaron, K. I. Peterson, D. Zolanz, W. Klemperer, F. J. Lovas, and R. D. Suenram, *J. Chem. Phys.* **92**, 7095 (1990).

<sup>19</sup>T. C. Germann and H. S. Gutowsky, *J. Chem. Phys.* **98**, 5235 (1993).

<sup>20</sup>M. Oldani, T.-K. Ha, and A. Bauder, *Chem. Phys. Lett.* **115**, 317 (1985).

<sup>21</sup>Calculated from results given by F. C. DeLucia, P. Helminger, and W. Gordy, *Phys. Rev. A* **8**, 2785 (1973).

<sup>22</sup>J. Plíva and A. S. Pine, *J. Mol. Spectrosc.* **93**, 209 (1982); J. Plíva, A. Valentin, J. Chazelas, and L. Henry, *ibid.* **134**, 220 (1989).

<sup>23</sup>R. L. Cook, F. C. DeLucia, and P. Helminger, *J. Mol. Spectrosc.* **53**, 62 (1974).

- <sup>24</sup>R. C. Cohen, K. L. Busarow, K. B. Laughlin, G. A. Blake, H. Havenith, Y. T. Lee, and R. J. Saykally, *J. Chem. Phys.* **89**, 4494 (1988).
- <sup>25</sup>R. C. Cohen, K. L. Busarow, and R. J. Saykally, *J. Chem. Phys.* **92**, 169 (1990).
- <sup>26</sup>M. D. Harmony *et al.*, *J. Phys. Chem. Ref. Data* **8**, 619 (1979).
- <sup>27</sup>J. A. Shea and W. H. Flygare, *J. Chem. Phys.* **76**, 4857 (1982).
- <sup>28</sup>C. H. Townes and A. L. Schawlow, *Microwave Spectroscopy* (McGraw-Hill, New York, 1955), Table 4-2.